Stable single-walled carbon nanotube-streptavidin complex for biorecognition

Liu, Z.; Galli, F.; Janssen, K.G.H.; Jiang, L.; Linden, H.J. van der; Geus, D.C. de; ... ; Abrahams, J.P.

Stable Single-Walled Carbon Nanotube−Streptavidin Complex for Biorecognition

Zunfeng Liu,*,† Federica Galli,‡ Kjeld G. H. Janssen,§ Linhua Jiang,† Heiko J. van der Linden,§ Daniël C. de Geus,† Patrick Voskamp,† Maxim E. Kuil,† René C. L. Olsthoorn,|| Tjerk. H. Oosterkamp,‡ Thomas Hankemeier,§ and Jan Pieter Abrahams*,†

Department of Biophysical Structural Chemistry, Leiden Institute of Chemistry, Gorlaeus Laboratories, Leiden University, P.O. Box 9502, 2300 RA Leiden, The Netherlands, Leiden Institute of Physics, 2333CA Leiden, University of Leiden, The Netherlands, Department of Analytical Biosciences, University of Leiden, P.O. Box 9502, 2300 RA Leiden, The Netherlands, Leiden Institute of Chemistry, LIC/Molecular Genetics, 2300 RA Leiden, The Netherlands

Received: December 2, 2009; Revised Manuscript Received: February 2, 2010

A novel method is described for preparing single walled carbon nanotube (SWNT)−streptavidin complexes via the biotin−streptavidin recognition. The complex shows stability in 18 days, strong biotin recognition capability, and excellent loading capacity (about 1 streptavidin tetramer per 20 nm of SWNT). Capturing biotinylated DNA, fluorophores, and Au nanoparticles (NPs) on the SWNT−streptavidin complexes demonstrates their usefulness as a docking matrix, for instance for electron microscopy studies, a technique requiring a virtually electron transparent support.

1. Introduction

Integration of biotechnology and nanotechnology provides new functional hybrid materials that incorporate the highly specific interaction and catalytic properties of biomolecules with the electronic, photonic, and chemical properties of nanomaterials.[1,2] Biomolecule recognition systems can modify and improve the nanomaterials' self-assembly capabilities, allowing the formation of supramolecular hybrid architectures that have potential applications such as sensors or nanoscale devices in proteomics, diagnostics, therapy, etc.[3] For successful application of many bionanohybrids, the stability of the specific recognition of target molecules is a critical issue.

The remarkable biomolecular recognition between the homotetrameric protein streptavidin and the water-soluble small molecule biotin is characterized by the extraordinary high affinity constant of the streptavidin−biotin interaction of $\sim 10^{14}$ $dm^3\ mol^{-1}$, the strongest ligand−receptor interaction currently known.[4] Because of the chemical and thermal stability of streptavidin and the relative ease with which target molecules can be biotinylated, the streptavidin−biotin affinity interaction is one of the most popular biological recognition pairs for bionano hybridization, both in commercial products and academic research.[5] Biomolecular recognition systems based on single walled carbon nanotubes (SWNTs) are especially attractive because of their extraordinary physical and chemical properties. The small diameter (1 nm) and tunable length (up to several micrometers) of SWNTs make them an ideal candidate for trace amount sensing, even for single molecule analysis. For instance, large molecular complexes captured by SWNT−streptavidin may allow straightforward analysis by transmission electron microscopy, in view of the high electron transparency of the SWNTs, if such a support would have been available, we could, for instance, have analyzed ribosomal complexes carrying the heat shock protein Hsp15 immediately in the microscope after having captured them on SWNT−streptavidin with biotinylated mRNA or biotinylated Hsp15. This would have avoided a tedious purification procedure and would have speeded up the project significantly.[6]

SWNTs are ideal substrates for building complex architectures. Their one-dimensional structure and specific electronic properties[7] allowed the preparation of chemical or biological sensors.[8−10] These studies indicate that carbon nanotubes based biosensors and bioreactors have a higher efficiency compared to glass carbon material due to their high surface to volume ratio/surface area.[11,12] The ease of functionalization of SWNTs allows the introduction of different functional or reactive groups along their one-dimensional structure, (e.g., −COOH groups can be introduced by HNO_3 oxidation), allowing stable complex formation by covalent bonding.[13] Because of the extraordinary strength and flexibility, SWNTs were also used as atomic force microscopy (AFM) tips for biological imaging by conjugating with biorecognition system.[14] The SWNT based biological complexes are used in vivo or in vitro for drug delivery, bioimaging, and biosensing.[15−21]

Different methods such as physisorption[22,23] and chemical linking[12] are used to attach streptavidin to SWNTs. Immobilization of streptavidin on SWNTs via physisorption relies on nonspecific hydrophobic interactions between SWNTs and streptavidin. Unfortunately, the SWNT−streptavidin complex is unstable: the streptavidin can dissociate from the SWNTs surface.[24] Covalent coupling through reactive groups ($-NH_2$ group, for instance) of the amino acid side-chains of streptavidin is frequently used for tethering streptavidin to SWNTs, for instance through carbodiimide cross linking.[12,25] Such chemical reactions are not very selective, may lead to heterogeneous attachment and involve residues required for function, and thus may affect the activity of the protein.[5] Moreover, there is still no conclusive evidence showing that such carbodiimide cross linking could significantly improve protein immobilization on carbon nanotubes above the level of adsorption.[26] Therefore

* To whom correspondence should be addressed. E-mail: liuz2@chem.leidenuniv.nl (Z.L.); abrahams@chem.leidenuniv.nl (J.P.A.). Phone: +31 (0)71 527 5666. Fax: +31 (0)71 527 4357.
† Department of Biophysical Structural Chemistry, Leiden Institute of Chemistry.
‡ Leiden Institute of Physics, University of Leiden.
§ Department of Analytical Biosciences, University of Leiden.
|| Leiden Institute of Chemistry, LIC/Molecular Genetics.

10.1021/jp911441d
Published on Web 02/19/2010

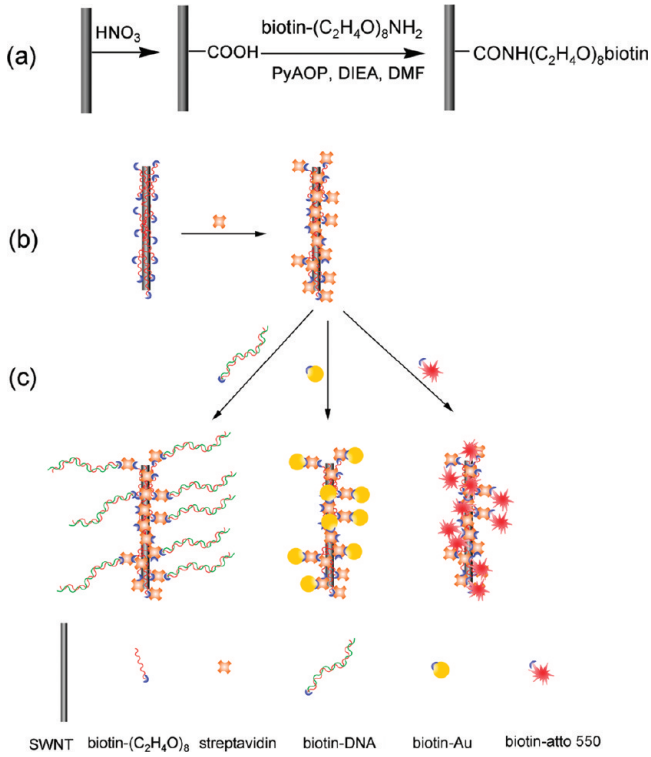

Figure 1. (a) Reaction scheme of the biotinylation of SWNTs, (b) schematic representation of the preparation of SWNT−streptavidin complexes via the biotin−streptavidin interaction, (c) schematic representation of preparation of SWNT−DNA, SWNT−Au, and SWNT−atto 550 NP complexes using SWNT−streptavidin as the docking matrix via biotin−streptavidin recognition.

more powerful capturing techniques that can stably and efficiently tether streptavidin to SWNTs are required.

Biotin binds to the streptavidin tetramer in 4:1 stoichiochemistry.[27] This enables sandwich binding architectures on SWNTs, i.e., [biotinylated SWNT]−[streptavidin]−[biotinylated species of interest]. Biotin shows stable chemical properties and can go through relatively harsh reaction conditions in different solvents, which allows biotinylation of SWNTs through a variety of routes and allows the introduction of other functional elements such as a PEG segment for preventing the nonspecific absorption.

In this paper, SWNTs were biotinylated via the coupling reaction between $-NH_2$ of an amine-terminated biotin (*O*-(2-aminoethyl)-*O*′-[2-(biotinylamino)ethyl]octaethylene glycol, biotin-PEG_8-NH_2) and −COOH group of SWNT-COOH, as shown in Figure 1a. A short segment of $(CH_2CH_2O)_8$ (PEG_8) is introduced between the SWNTs and biotin in order to render the SWNTs soluble in H_2O; it also serves as a spacer, decreasing the steric hindrance between the SWNTs and streptavidin and the nonspecific binding between SWNTs and proteins. The biotinylated SWNT are soluble in H_2O without any detergent, which can be attributed to the PEG_8 unit.

Biotinylated SWNT in H_2O can interact with streptavidin to form SWNT−strepatavidin complexes, as shown in Figure 1b. Note that the assembly of biotinylated SWNT and streptavidin is a cross-linking aggregation system, because the functionality of both the biotinylated SWNT (≫2) and streptavidin (4) is larger than 2, as in typical cross-linking polymerization system.[28,29] Similar cross-linking aggregation has been reported for the self-assembly of the biotinylated Au nanopartices (NPs) and streptavidin, in which the aggregation of the Au NPs resulted in a nonordered three-dimensional network of NPs.[30,31] It was found that the size of the aggregates and the formation rate depend on the relative concentrations of each species.[30,32] Therefore, in order to obtain an effective self-assembly of biotinylated SWNT and streptavidin, a careful control of the experimental details is required to eliminate cross-linking between SWNTs and streptavidin. Three critical conditions of this cross-linking aggregation system are described in Figure 2. In Figure 2a, comparable amounts of functional SWNT immobilized biotin groups and streptavidin are used. In this case, strong cross-linking of SWNTs will occur and a three-dimensional network structure will be formed. In theory, a large aggregate of SWNTs will eventually be formed under this condition. In Figure 2b, an excess amount of SWNTs dominates the mixture; here, the amount of streptavidin is so limiting that the SWNTs cannot be linked together. On the contrary, the biotin-binding sites in streptavidin may be more easily filled by biotin moieties from the same SWNT, as these are more accessible to the streptavidin than those from other SWNT. Therefore, the cross-linking between SWNTs can be prevented and an aggregation structure of "intramolecular cross-linking" between SWNTs and streptavidin and/or a SWNT-branch/streptavidin-core structure can be formed. There will be no active biotin-binding sites on the SWNT−streptavidin complexes in this situation. In Figure 2c, an excess amount of streptavidin is used in the mixture. In contrast to the case in Figure 2b, the SWNTs are surrounded by streptavidin molecules, the biotin moieties on SWNT are easily bound by different streptavidin molecules and the SWNTs will hardly be cross-linked because they are separated by the surrounding streptavidin molecules. Finally, streptavidin-branch/SWNT-core complexes will be formed and there are still active biotin-binding sites in the SWNT−streptavidin complex. Hence, a small amount of biotinylated SWNT and an excess of streptavidin should be used for self-assembly of the SWNT−streptavidin affinity matrix.

To investigate the biotin-binding activity of the SWNT−streptavidin complexes prepared in this paper, different biotinylated species such as biotinylated DNA, biotinylated fluorophore, and biotinylated Au NPs were used, as shown in Figure 1c. Such complexes of SWNT−DNA,[7,33] SWNT−Au NP,[34] SWNT−fluorophores,[15] and multifunctional sensors based on simple complexes[17,35] have attractive properties and applications. For example, conjugates of DNA with SWNTs have potential applications in gene therapy,[15] multidimensional devices,[1,3] and nanobiotechnology.[2,5] CNTs functionalized with fluorophores can be visualized in biological environments using conventional fluorescence microscopy.[36,37] Metal or metal compound NPs were conjugated to SWNTs in order to obtain novel properties or explore new applications:[2] SWNT−Au−SWNT junctions were prepared by self-assembly[34] and quantum dot−SWNT[18] were prepared for cell imaging.

In this paper, a biotinylated DNA having 1000 base pairs, a biotinylated fluorophore atto 550, and biotinylated Au NPs were used to interact with the SWNT−streptavidin complex to form SWNT−DNA, SWNT−atto 550, and SWNT−Au NP conjugates. We investigated these complexes with AFM, which required them to be immobilized on mica. However, because DNA is negatively charged, it does not stick to the mica surface and is easily removed by rinsing with H_2O. Therefore, we prepared a SWNT−streptavidin coated mica surface and then incubated it with a biotinylated DNA solution to prepare the SWNT−DNA conjugates. This method rolls the synthesis, purification, and AFM imaging of the SWNT−DNA conjugate into a single step. The same preparation procedure was used for synthesis of SWNT−atto 550 and SWNT−Au NP conjugates.

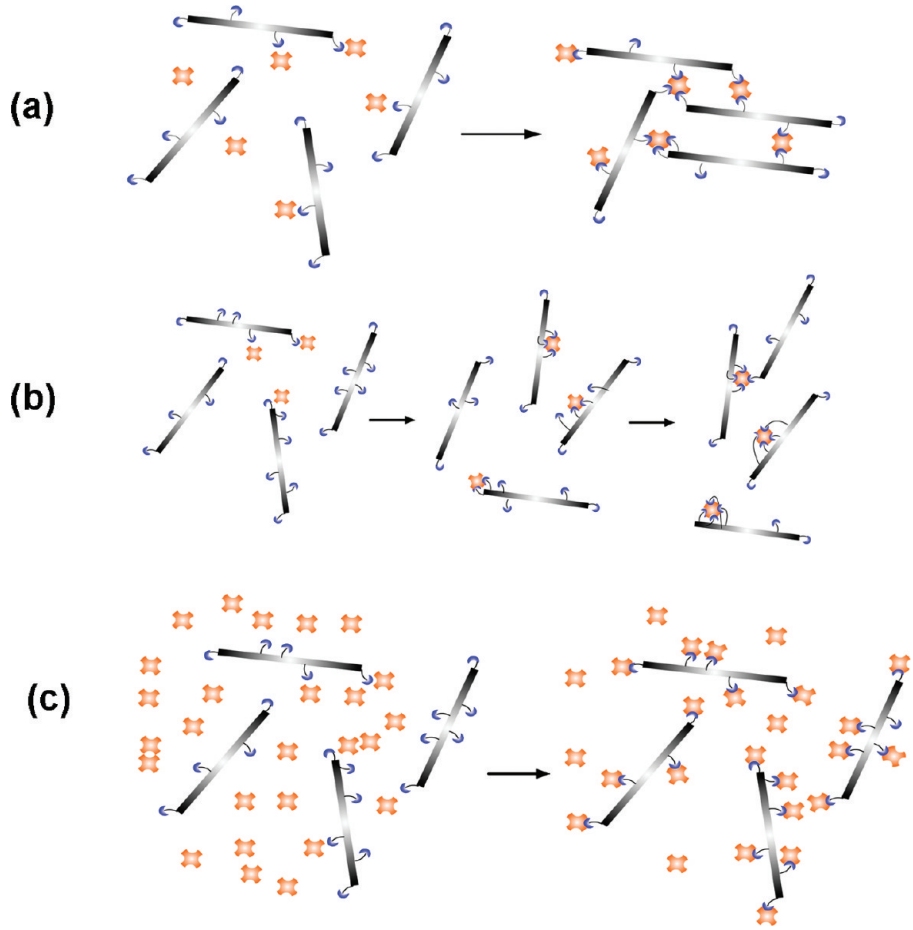

Figure 2. Schematic representation of the cross-linking aggregation system of biotinylated SWNT with streptavidin in different critical conditions: (a) comparable amounts of SWNT immobilized biotin and streptavidin, (b) excess amount of biotinylated SWNT compared to streptavidin, and (c) excess amount of streptavidin compared to biotinylated SWNT.

2. Experimental Section

2.1. Materials. HIPCO SWNTs (Lot no. SP0295) were purchased from Unidym, Inc. Streptavidin was purchased from ProSpec-Tany TechnoGene Ltd. (7-Azabenzotriazol-1-yloxy)-tripyrrolidinophosphonium hexafluorophosphate (PyAOP, 96%), *N*,*N*-diisopropylethylamine (99.5%, biotech. grade), *O*-(2-aminoethyl)-*O*′-[2-(biotinylamino)ethyl]octaethylene glycol (biotin-PEG_8-NH_2, ≥95% oligomer purity, the number 8 means that the repeated $-CH_2CH_2O-$ unit is 8), *O*-(2-aminoethyl)-*O*′-[2-(boc-amino)ethyl]octaethylene glycol (PEG_8-NH_2, ≥95% oligomer purity), 3-aminopropyltriethanoxysilane (APTES), atto 550, and biotinylated atto 550 were purchased from Sigma-Aldrich. Biotinylated Au NPs (average diameter of 5 nm, 0.01% based on Au) were purchased from NanoCS INC. DMF (99.8%) was purchased from Biosolve Ltd. Bio-Rad protein dye (#500−0002EDU) was purchased from Bio-Rad Ltd.

2.2. Preparation of SWNT−Streptavidin Complexes. The SWNTs (20 mg) were sonicated for 10 min in Milli-Q H_2O (15 mL) using a tip sonicator (Sonics and Materials Inc., Model VCX 750, 750 W) working at 24% amplitude, and then HNO_3 (65%, 16 mL) and Milli-Q H_2O (70 mL) were added. The mixture was refluxed at 120 °C for 2 h with magnetic stirring. (Different reflux times were used for other oxidation conditions.) This process was repeated twice to obtain individualized SWNT with little fragmentation (see Figure S5 of Supporting Information) and introduced −COOH groups onto the defects of tube sidewall and ends. Then the SWNT-COOH were membrane filtered (Hydrophilic, Tianjin Autoscience Ltd., 0.22 μm) and washed twice with NaOH (10 mM), HCl (10 mM), and Milli-Q H_2O. This SWNT-COOH preparation was vacuum-dried at 80 °C for 72 h (yield: 14 mg).

SWNT-COOH (2.5 mg) was dispersed in DMF (1 mL, dried with molecule sieve (4 Å) overnight), then Biotin-PEG_8-NH_2 (50 mg), PyAOP (38 mg), and DIEA (18.9 mg) were added. The mixture was stirred for 1 h and then membrane filtered (Nylon, 0.22 μm, Tianjin Autoscience Ltd.) and washed thoroughly with DMF and transferred to Milli-Q H_2O. The product is referred to "SWNT-biotin" below. There are some insoluble SWNT aggregates produced during this process, which can be removed by centrifuging at 7000 rpm for 30 min. The SWNT assay indicated the yield of SWNT in the supernatant to be ∼0.6 mg. The synthesis of SWNT-PEG_8 without the biotin moiety is analogous to the above procedure.

The SWNT−biotin solution in Milli-Q (0.02 mg mL^{-1}, 10 mL) was added to a streptavidin solution (1 mg mL^{-1}, 10 mL) in PBS (phosphate buffered saline, pH 7.2,) dropwise with shaking, and then mixed for 30 min at 40 rpm using a roller mixer (Stuart, model STR9D). Then the mixture was washed 3 times using a centrifugal filter (Amicon Ultra-15, 100 K), and dispersed in Milli-Q H_2O (5 mL). The product was marked as SWNT−streptavidin. The control experiment of SWNT-PEG_8 complexing with streptavidin was the same as the above procedure.

2.3. Preparation of DNA, SWNT−DNA, SWNT−atto 550, SWNT−Au NP Conjugates. The biotinylated 1000-bps DNA was obtained by a polymerase chain reaction (PCR) using primers ZUN-1 (5′Bio-GTAATACGACTCACTATAGGCTA-GCCACCATG-3′) and ZUN-4 (5′-CGATAAGCTTGATATC-

GAATTCCTGCAGCCCGG-3′) and plasmid pRLHL as template. To obtain the nonbiotinylated 1000-bps DNA, primer ZUN-1 was replaced by one without biotin (ZUN-2). The resulting DNA fragments were purified over Micro Bio-Spin 6 chromatography columns (Bio-Rad, Hercules, CA).

SWNT−streptavidin complexes (0.05 mg mL^{-1} for SWNT assay) were deposited on freshly cleaved mica for 10 min, then rinsed several times with water and dried gently under a stream of nitrogen gas. Then biotinylated DNA (20 μg mL^{-1}), biotinylated atto 550 (0.01 mg mL^{-1}), or biotinylated Au NPs (0.1 mg mL^{-1} based on Au) were deposited on the SWNT−streptavidin complexes coated in mica for 30 min at room temperature for the preparation of SWNT−DNA, SWNT−atto 550, or SWNT−Au NP. After incubation, the mica was rinsed several times with water and dried gently under a stream of nitrogen gas. The control experiment of SWNT−streptavidin complexing with non biotinylated DNA was performed analogous. The control experiment of SWNTs complexing with atto 550 was carried out on APTES treated mica.

2.4. Measurements (AFM, Fourier Transform Infrared (FTIR), Fluorescence Microcopy (FM), and UV−Vis Spectroscopy). Tapping mode at 300 Hz was used to acquire the AFM images under ambient conditions (AFM: Digital Instruments Dimension 3100). The tip diameter of the cantilever was ~10 to ~20 nm. Samples of SWNT−streptavidin, SWNT−DNA, and SWNT−Au NP complexes were prepared as described above. FTIR spectroscopy measurements were performed at ambient conditions using a Perkin-Elmer FTIR spectrometer (Paragon 1000). Samples for FTIR were prepared with KBr to form transparent pellets. Confocal microscopy (Olympus BX51TF) was used to collect fluorescent images of SWNT−atto 550 complexes after excitation at 488 nm using an argon laser. UV−vis spectrophotometry (Varian Cary 50 series) was used to obtain the spectrum of SWNTs and streptavidin. UV−vis spectrophotometry (Ultrospec 110 Pro) was also used to obtain the absorbance value of SWNTs, SWNT−biotin, and SWNT−streptavidin complexes at 595 nm, required for measuring the concentration of SWNTs, the experimental details are shown in Figure S6 of Supporting Information.

2.5. Acid−Base Titration and Streptavidin Concentration Determination via Bradford Assay. The mole percentage of the −COOH groups on SWNTs was determined using acid−base titration.[38,39] SWNT-COOH (14.34 mg) was dispersed in 25 mL of H_2O and then mixed with $NaHCO_3$ (10 mM, 25 mL) and stirred for 24 h under Ar protection. The above two solutions were degassed in a vacuum and sonicated for 15 min in order to remove the CO_2 in solution before being mixed together. Then the reaction mixture was filtered through a 0.22 μm membrane. HCl acid (5 mM, 50 mL) was added to the filtrate and mixed for 15 min by shaking, and the same degassing was carried out to remove the CO_2 in solution. Then the solution was titrated (using a pH meter, inoLab pH 720) to pH = 7.0 under Ar protection, with 2.08 mL of NaOH (5 mM).

The loading extent of streptavidin on SWNT in the SWNT−streptavidin complexes was determined by measuring the streptavidin concentration and SWNT concentration, respectively. The streptavidin concentration was measured using a Bradford assay,[40] with soluble streptavidin as the standard. Measurements of every sample were made in duplicate, and in order to eliminate the influence of SWNTs, the standard contains the same concentration of SWNTs as in the target sample. The experimental details are shown in Table S1 of Supporting Information.

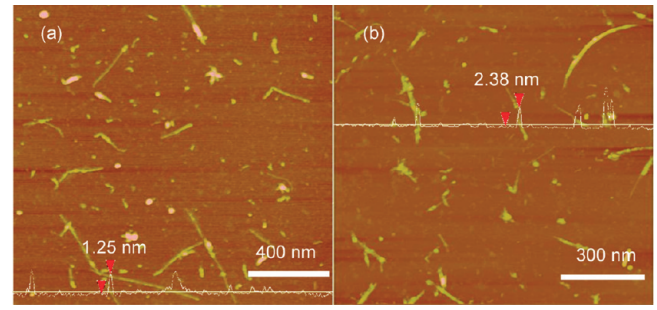

Figure 3. AFM images of (a) SWNT-COOH and (b) biotinylated SWNT. The cross-section analysis shows a diameter of 1.25 nm for SWNT-COOH and of 2.38 nm for biotinylated SWNT.

3. Results and Discussion

3.1. Biotinylation of SWNT. Figure 3 shows AFM images of SWNT-COOH and the biotinylated SWNT. The SWNT-COOH was prepared by boiling the raw SWNTs in 2.6 M nitric acid for 2 h twice. The oxidation of SWNTs has been investigated in numerous studies,[41−44] using agents such as HNO_3 (2.6 M and 8M), mixture acid of HNO_3/H_2SO_4, $KMNO_4$/KOH, etc.[45] It was reported that the mild oxidation (e.g., HNO_3, 2.6 M) tends to introduce the −COOH groups on the tube ends and at the defect sites of the sidewall but does not create new defects.[41,43] Therefore, the −COOH content of SWNTs remains constant after all the defects have been carboxylated.[43] Small fragments can be produced in this mild oxidation and their amount tends to increase with time.[44] In the view of the applications of SWNTs in biorecognition systems we have in mind, we hope to (1) obtain individualized SWNT, (2) introduce −COOH groups on the SWNTs and then render them soluble, and (3) produce as few fragments as possible during this oxidation process. Therefore, we investigated different oxidation times, ranging from 2 to 15 h, shown as AFM images in Figure S5 of Supporting Information. It was found that the 4 h oxidation was best. Short-duration oxidation (2 h, e.g.) was not sufficient to debundle the SWNTs, while longer-duration oxidation (e.g., >4 h) produced a lot of fragments. Similar results are reported in the literature.[44] To obtain sufficient debundling of SWNTs, we also tested twice repeated 2 h oxidation, with a sonication process in between. As expected, the twice repeated 2 h oxidation was the optimized oxidation condition in this paper.

This procedure cut down the SWNTs into short, individualized tubes having a length distribution of several hundred nanometers and diameter distribution of ~1 nm, as shown in Figure 3a (see also Figure S1 of Supporting Information for statistical analysis of length and diameter distributions). The −COOH groups that were introduced during this HNO_3 oxidation process can be observed as a weak peak at 1736 cm^{-1} in the FTIR spectrum in Figure 4. The mole percentage of the −COOH groups on SWNTs was determined using acid−base titration.[38,39] SWNT-COOH (14.34 mg) reacted with $NaHCO_3$ (10 mM, 25 mL) and formed SWNT-COO^-Na^+. Then HCl acid (5 mM, 50 mL) reacted with the remaining $NaHCO_3$. The remaining HCl acid was titrated to pH = 7.0 with NaOH (5 mM). As the same molar amounts of $NaHCO_3$ and HCl were used, the molar amount of −COOH groups should be equal to that of the consumed NaOH (5 mM, 2.08 mL). The molar percentage of −COOH groups on SWNTs was calculated to be 0.9%, corresponding to 4.8% mass percentage.

After biotinylation, the SWNTs had diameters of ~2−5 nm (see Figure S1 of Supporting Informtion for statistical analysis). The cross-section analysis in Figure 3b shows a typical biotinylated nanotube having a diameter of 2.38 nm. The

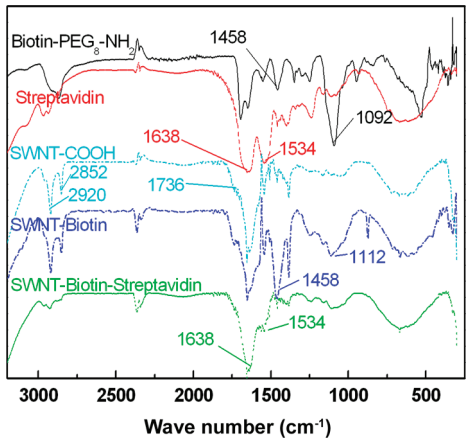

Figure 4. FTIR of biotin-PEG_8-NH_2, streptavidin, SWNT-COOH, SWNT−biotin, and SWNT−streptavidin in the range of 3000−500 cm^{-1}.

diameter increase of SWNTs after biotinylation can be attributed to the linking of biotin-PEG_8 segment onto the SWNTs as well as the aggregation of SWNTs during the biotinylation process. The possible reason might be that the biotin-PEG_8-NH_2 may contain some impurities such as NH_2-PEG_8-NH_2, which would serve as a cross-linker of SWNTs in the reaction system. We also found that not all of the SWNTs were soluble after the biotinylation process, and we removed these insoluble aggregates by centrifugation. After the biotinylation process, the length distribution was almost unchanged, as can be seen in Figure S1 of Supporting Information. The FTIR spectra in Figure 4 confirm the presence of the biotin-PEG_8-NH_2, with peaks at 1458 cm^{-1} (corresponding to CH_2 bending) and at 1092 cm^{-1} (corresponding to the vibration of the ether group in the PEG segment), which also exist in the FTIR spectrum of SWNT-biotin (1458 and 1112 cm^{-1}).

3.2. Preparation of SWNT−Streptavidin Complexes. By carefully adding a dilute biotinylated SWNT (0.02 mg mL^{-1}, 10 mL) solution dropwise into a streptavidin solution (1 mg mL^{-1}, 10 mL) followed by through washing, a complex of SWNT−streptavidin with the SWNT fully covered by streptavidin was synthesized. Figure 5a shows the AFM image of SWNT−streptavidin complexes, about 16 h after preparation. The SWNTs were fully covered with streptavidin molecules, as indicated by the cross-section analysis in the zoomed-in image (Figure 5b), which shows a typical complex having a diameter of ∼7 nm. The diameter distribution of the SWNT−streptavidin complexes is mainly in the range from 5−15 nm, as shown in the statistical analysis in Figure S1 of Supporting Information. The increase in the diameter of the SWNT−streptavidin complexes compared to the biotinylated SWNT can be attributed to the attachment of streptavidin molecules to the SWNTs. The FTIR spectrum of the SWNT−streptavidin complexes in Figure 4 also confirms the presence of streptavidin. Streptavidin shows strong peaks at 1638 cm^{-1} (corresponding to amide I: −C═O stretch of protein) and 1534 cm^{-1} (corresponding to amide II: −C−N stretch and −C−N−H deformation), which were also present in the FTIR spectrum of SWNT−streptavidin complexes. By use of a Bradford assay, we determined the loading extent of streptavidin on SWNT as 1.2 mg of streptavidin per mg of SWNT. The experimental details and results are shown in Table S1 and Figure S2 of Supporting Information, respectively. By assuming all of the atoms of SWNT are carbon, the mole percentage of streptavidin molecules on carbon atoms relative to SWNT is 0.024%. As discussed previously, the mole percentage of the −COOH groups relative to SWNT was

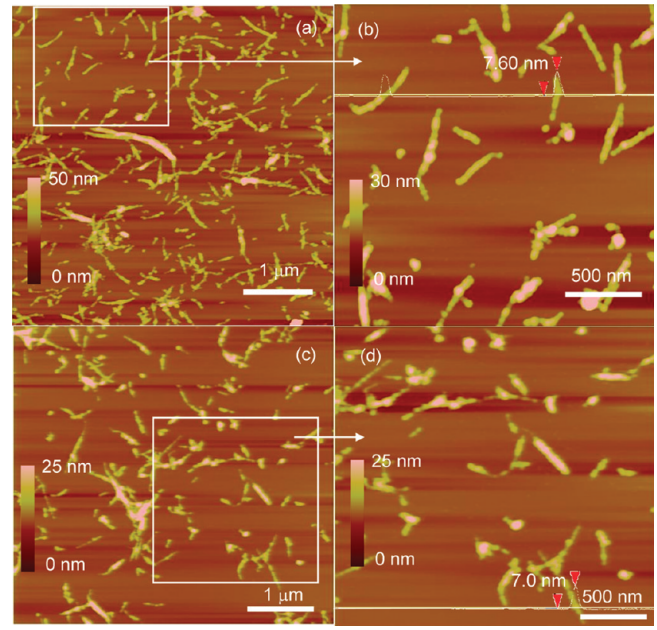

Figure 5. AFM images of SWNT−streptavidin complexes (a), the zoomed-in image (b), 18 days after preparation (c), and the zoomed-in image (d). The cross-section analysis indicates the diameter of a SWNT−streptavidin complex to be ∼7 nm, irrespective of whether the sample was freshly prepared or 18 days after the preparation.

determined to be 0.90%; therefore, about 2.7% of the −COOH groups on SWNT were linked with streptavidin. By calculating the average diameter of the SWNT below 3 nm in Figure S1 of Supporting Information, we got an average diameter of ∼1.3 nm for the SWNT. The perimeter of the circular cross-section of the SWNT is $\pi \times 1.3 = 4.1$ nm. By assumption that the C−C bond length is 0.14 nm, there are $4.1/0.14 \approx 29$ carbon atoms on the cross section. As there are 2.4 streptavidin molecules attached to 10000 carbon atoms on a SWNT, the average distance between two streptavidin molecules on a SWNT is $10000 \times 0.14/(29 \times 2.4) \approx 20$ nm. An occupancy of 1 streptavidin tetramer per 20 nm of SWNT is in line with a high coverage of the SWNT.

Figure 5 shows that most SWNTs exist as separate tubes, and a few SWNTs are connected to one another forming a branched structure, but almost no three-dimensional cross-linked structures were observed. This was achieved by adding a vast excess of streptavidin, achieving ligation of all the biotin moieties of the SWNT with separate streptavidin molecules (see also Figure 2c). Cross-linking structures will be formed at lower amounts of streptavidin. We added a dilute biotinylated SWNT (0.02 mg mL^{-1}, 10 mL) solution dropwise into a streptavidin solution (0.1 mg mL^{-1}, 10 mL), followed by thorough washing. As a result, the strong cross-linking happens between biotinylated SWNT and streptavidin, as shown in Figure S3 of Supporting Information, corresponding to Figure 2b. We further decreased the amount of streptavidin and made a SWNT-rich system by dropwise adding 1 mL of streptavidin solution (10^{-4} mg mL^{-1}) into SWNTs (0.02 mg mL^{-1}, 3 mL). As a result, a SWNT branch/streptavidin core structure corresponding to Figure 2a was formed, as shown in Figure S3 of Supporting Information.

Note that unlike SWNT−streptavidin complexes reported in the literature that are formed via nonspecific absorption (where there are always unbound streptavidin molecules in the image[22,24]), all streptavidin molecules in parts a and b of Figure 5 are ligated and none occur separate from the SWNTs. This indicates that

all unligated streptavidin molecules were removed by repeated filtration and that almost no streptavidin molecules dissociated from the SWNT−streptavidin complexes during the overnight incubation. The surface properties of the SWNT−streptavidin complexes are fully altered compared to the undecorated SWNTs, because of the high coverage of the streptavidin on the SWNT. The SWNT-COOH and the biotinylated SWNT did not stick to the pure mica surface but could be absorbed tightly on an APTES treated mica surface by the interaction between the amine groups and the SWNT sidewall. In contrast, the SWNT−streptavidin complexes could not be absorbed on APTES treated mica but did stick tightly to the untreated mica surface. The observed absorption of the SWNT−streptavidin complex onto the mica surface can be attributed to the electrostatic binding between streptavidin and mica.[46,47] It was reported that the streptavidin in H_2O strongly absorbs on mica surfaces, which can be inhibited by adding monovalent cations.[47] To show that the streptavidin was specifically complexed to biotinylated SWNT, we did a control experiment using SWNT-PEG_8 without a biotin moiety. The SWNT-PEG_8 complexes were synthesized using the same method as SWNT-PEG_8-biotin, and the SWNT-PEG_8 (0.02 mg mL^{-1}, 10 mL) was added dropwise into a streptavidin solution (1 mg mL^{-1}, 10 mL) followed by thorough washing. The AFM images of SWNT-PEG_8 before and after "complexing" with streptavidin are shown in Figure S4 of Supporting Information. It can be seen that almost no streptavidin molecules are attached on the SWNT-PEG_8. Also, it should be noted that both the images are taken on APTES-treated mica surface, and neither of the preparations can stick to the pure mica surface, indicating the failure of streptavidin complexing with the SWNT-PEG_8.

We also investigated the stability of the SWNT−streptavidin complexes over 18 days, the AFM imaging 18 days after preparation are shown in Figure 5c. The SWNTs were still wrapped with proteins and there were no free streptavidin molecules, indicating that streptavidin molecules did not dissociate from the complex. Figure S1 of Supporting Information show the statistical analysis of the length and diameter distributions of the SWNT−streptavidin complexes, which almost did not change compared with the freshly prepared one. The cross-section analysis of a zoomed-in image (Figure 5d) shows a typical complex with a diameter of ∼7 nm. This indicated that the complex was stable over 18 days, unlike the SWNT−streptavidin complexes formed via nonspecific binding, which were reported to dissociate upon repeated dialysis.[24] The stability of the complex over 18 days indicated that all streptavidin molecules bound to the SWNT via the specific biotin−streptavidin interaction. We postulate that: (1) the high coverage of biotin-bound streptavidin on SWNT competes with the nonspecific absorption of streptavidin on SWNT; (2) the PEG_8 spacer segment decreases the nonspecific binding of the streptavidin to SWNT; (3) the repeated filtration process removed the unbound streptavidin molecules.

3.3. SWNT−DNA, SWNT−Fluorophore, and SWNT−Au NP Conjugates. Figure 6 shows the AFM images of the SWNT−DNA conjugates. Almost all of the SWNT−streptavidin complexes linked to a multitude DNA strands (parts a and c of Figure 6). This indicated a good biotin-binding ability and high biotin-loading capacity of the SWNT−streptavidin complexes. The zoomed-in images (parts b and d of Figure 6) suggest that the loading of DNA strands on a single SWNT was so high that they criss-crossed or compactly stacked onto one another. They were not evenly dispersed on both sides of the SWNT, which may have been caused by the H_2O rinsing and subsquent

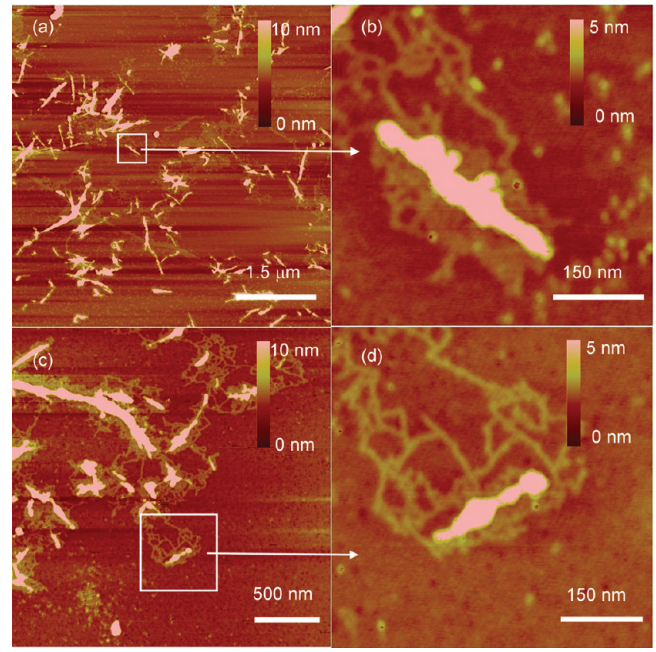

Figure 6. AFM images of SWNT−DNA conjugates prepared via the biotin−streptavidin affinity interaction, using SWNT−streptavidin complexes as the docking matrix (a) and (c) and the zoomed-in images (b) and (d).

N_2 blow-drying procedure. This high loading with DNA strands also reflected the high coverage of streptavidin on the SWNT. As far as we know, this is the highest loading of DNA strands onto the SWNT visualized with AFM reported so far. The compact stacking may be due to the extended aggregation, perhaps enhanced by Marangoni effects. To show that the biotin-DNA was linked to the SWNT via the specific streptavidin−biotin recognition, and not by nonspecific interactions, we performed a control experiment where DNA without a biotin tag was used. Not a single DNA strand was found that was linked to any SWNT−streptavidin complex (Figure S7 of Supporting Information).

The fluorescence image of the SWNT−atto 550 conjugates (a fluorescent dye) (Figure 7a) shows a strong specific signal. Biotinylated atto 550 on mica gave no signal (Figure 7b), indicating that the atto 550 does not specifically interact with mica. When we incubated the SWNT−streptavidin with unbiotinylated atto 550, there was a very weak signal (Figure 7c), which may be attributed to nonspecific interactions of atto 550 with the wall of SWNTs via $\pi-\pi$ interactions. It has been reported that although small organic fluorophores can interact with CNTs via $\pi-\pi$ interactions and form noncovalent assemblies[48] the charge/energy transfer from the fluorophores to the CNTs through these interactions results in fluorescence quenching and low quantum yields.[18] Therefore we did a control experiment of atto 550 on unmodified SWNTs, as shown in Figure 7d. It can be seen that there is faint signal in Figure 7d, which should be attributed to the atto 550 nonspecifically attaching to the SWNTs. Therefore, the strong, specific signal in Figure 7a most likely reflects the specific biotin−streptavidin interaction, rather than $\pi\pi$ bonding.

Parts a−c of Figure 8 show the AFM images of SWNT−Au NP conjugates in height, phase, and amplitude. The Au NPs have an average diameter of ∼5 nm, which is similar to that of streptavidin, as shown in the AFM image in Figure 9c and the diameter distribution in Figure 9d. To help distinguish the Au NPs, the height, phase, and amplitude images of the SWNT−

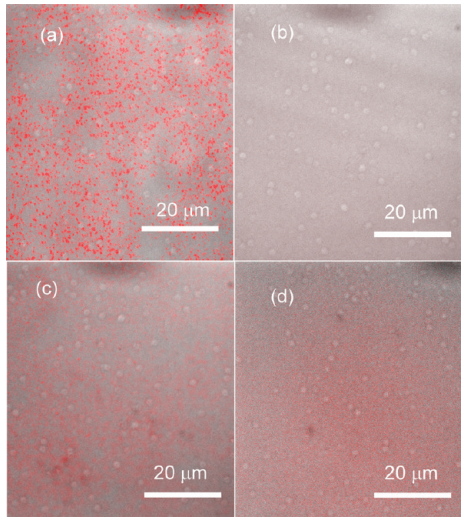

Figure 7. Fluorescence images of atto 550 biotin on SWNT−streptavidin complexes coated mica after washing with water (a), atto 550 biotin on mica after washing with water (b), atto 550 on SWNT−streptavidin complexes coated mica after washing with water (c), atto 550 on SWNTs coated mica-NH_2 after washing with water (d).

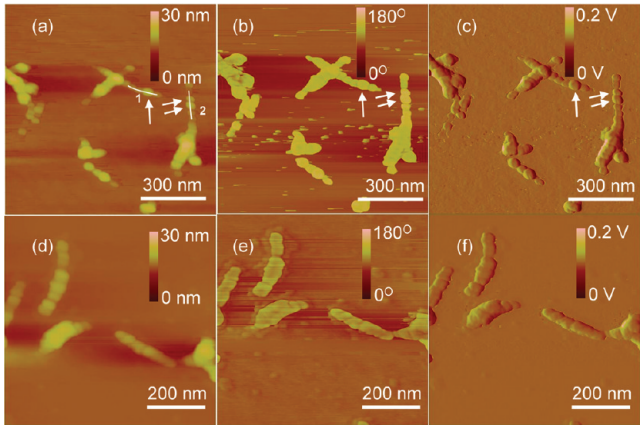

Figure 8. AFM images of SWNT−Au NP prepared from biotinylated Au NPs and SWNT−streptavidin complex in height (a), phase (b), and amplitude (c), and AFM images of SWNT−streptavidin in height (d), phase (e), and amplitude (f) as a comparison.

streptavidin complexes were measured as controls, for comparison with the SWNT−Au NP, as shown in parts d−f of Figure 8. In parts a−c of Figure 8, the arrows point out some NPs that had clear and sharp edges, which were clearly on the "ridge" of the SWNT−streptavidin complexes. No such NPs were observed in the SWNT−streptavidin complexes as shown in parts d−f of Figure 8. Therefore, such particles could be the Au NPs.

By use of the cross-section analysis[49] of the regions 1 and 2 pointed by the arrows, as shown in parts a and b of Figure 9, it can be seen the height between these particles is 3.6 (corresponding to the region 1), 3.3, and 4.2 nm (corresponding to region 2), in accordance with the diameter distribution of the Au NPs shown in Figure 9d.

4. Conclusions

We have devised a novel method for preparing SWNT−streptavidin complexes via the biotin−streptavidin interaction. The streptavidin is specifically tethered to the SWNT and the SWNT−streptavidin complexes show unique features such as very high loading of streptavidin and very high biotin-binding

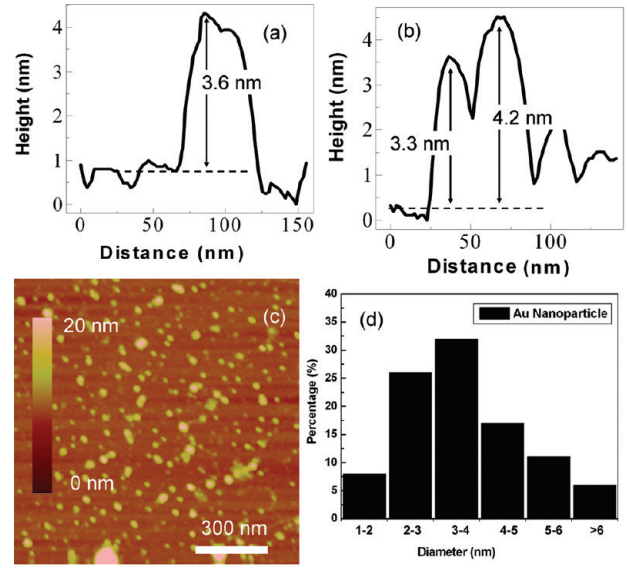

Figure 9. (a) Cross-section analysis of the location 1 in Figure 8a, (b) cross-section analysis of the location 2 in Figure 8b, (c) AFM image of Au NPs on mica, and (d) statistical analysis of the diameter distribution of the Au NPs by counting 100 particles.

capability, thus providing a versatile affinity scaffold. The SWNT−streptavidin complexes show stability of over 18 days. For long-term use, the stability over a longer period up to several months will be carried out in further investigations. The method provides a new generic tool for the construction of many different types of SWNT based complexes. It offers promising possibilities for assembling SWNT with biotinylated species, and multifunctional structures can be formed by combination with other methods. For example, the SWNT−streptavidin matrix may be used for fishing for biotinulated proteins and their complexes, for self-assembly using complementary ss-DNA strands, and for functionalization with multiple different groups. Compared to other affinity scaffolds, the SWNT−streptavidin complexes have the following advantages: they are very thin, therefore it can be used for TEM studies such as the single particle analysis; they may enter the living cells, and thus be used for gene/drug delivery; furthermore, they are easily made and relatively cheap, allowing bulk quantity preparations.

Acknowledgment. The authors gratefully acknowledge the financial support from Cyttron foundation (http://www.cyttron.org) and NWO Veni grant 2009 (Project Number: 700.59.407). We thank Raimond B. G. Ravelli, Gerda E. M. Lamers, and G. A. van Albada for technical support.

Supporting Information Available: Statistical analysis of diameter and length distributions of the AFM images of SWNTs, SWNTs-PEG_8-biotin, SWNTs−streptavidin, and SWNTs−streptavidin 18 days later, working curve of UV−vis absorption to concentration of streptavidin via the Bradford assay, feed ratio of determining the streptavidin loading on SWNTs via the Bradford assay, AFM images corresponding to cartoons in parts a and b of Figure 2, AFM images of the control experiments of SWNTs coated with the PEG_8 segment without the biotin moiety, AFM images of SWNTs treated with HNO_3 (2.6 M) for different time at 120 °C, UV−vis spectra of SWNTs in H_2O and streptavidin in PBS buffer, working curve of the absorption to the concentration of SWNTs at 595 nm, AFM images of the control experiment of SWNT-PEG-Biotin "complexing" with no biotinylated DNA. This material is available free of charge via the Internet at http://pubs.acs.org.

References and Notes

(1) Baron, R.; Willner, B.; Willner, I. *Chem. Commun.* **2007**, *4*, 323.
(2) Katz, E.; Willner, I. *Angew. Chem., Int. Ed.* **2004**, *43*, 6042.
(3) Niemeyer, C. M. *Angew. Chem., Int. Ed.* **2001**, *40*, 4128.
(4) Weber, P. C.; Ohlendorf, D. H.; Wendoloski, J. J.; Salemme, F. R. *Science* **1989**, *243*, 85.
(5) You, C.; Bhagawati, M.; Brecht, A.; Piehler, J. *Anal. Bioanal. Chem.* **2009**, *393*, 1563.
(6) Jiang, L. H.; Schaffitzel, C.; Bingel-Erlenmeyer, R.; Ban, N.; Korber, P.; Koning, R. I.; de Geus, D. C.; Plaisier, J. R.; Abrahams, J. P. *J. Mol. Biol.* **2009**, *386*, 1357.
(7) Lyonnais, S.; Goux-Capes, L.; Escude, C.; Cote, D.; Filoramo, A.; Bourgoin, J. P. *Small* **2008**, *4*, 442.
(8) Li, J.; Lu, Y. J.; Ye, Q.; Cinke, M.; Han, J.; Meyyappan, M. *Nano Lett.* **2003**, *3*, 929.
(9) Snow, E. S.; Perkins, F. K.; Houser, E. J.; Badescu, S. C.; Reinecke, T. L. *Science* **2005**, *307*, 1942.
(10) Star, A.; Gabriel, J. C.; Bradley, K.; Gruner, G. *Nano Lett.* **2003**, *3*, 459.
(11) Davis, J. J.; Green, M. L. H.; Allen, O. H.; Leung, Y. C.; Sadler, P. J.; Sloan, J.; Xavier, A. V.; Chi Tsang, S. *Inorg. Chim. Acta* **1998**, *272*, 261.
(12) Huang, W. J.; Taylor, S.; Fu, K. F.; Lin, Y.; Zhang, D. H.; Hanks, T. W.; Rao, A. M.; Sun, Y. P. *Nano Lett.* **2002**, *2*, 311.
(13) Banerjee, S.; Hemraj-Benny, T.; Wong, S. S. *Adv. Mater.* **2005**, *17*, 17.
(14) Wong, S. S.; Joselevich, E.; Woolley, A. T.; Cheung, C. L.; Lieber, C. M. *Nature* **1998**, *394*, 52.
(15) Kam, N. W. S.; Dai, H. J. *J. Am. Chem. Soc.* **2005**, *127*, 6021.
(16) Kam, N. W. S.; Jessop, T. C.; Wender, P. A.; Dai, H. J. *J. Am. Chem. Soc.* **2004**, *126*, 6850.
(17) Chen, R. J.; Bangsaruntip, S.; Drouvalakis, K. A.; Kam, N. W. S.; Shim, M.; Li, Y. M.; Kim, W.; Utz, P. J.; Dai, H. J. *Proc. Natl. Acad. Sci. U. S. A.* **2003**, *100*, 4984.
(18) Bottini, M.; Cerignoli, F.; Dawson, M. I.; Magrini, A.; Rosato, N.; Mustelin, T. *Biomacromolecules* **2006**, *7*, 2259.
(19) Kam, N. W. S.; O'Connell, M.; Wisdom, J. A.; Dai, H. J. *Proc. Natl. Acad. Sci. U. S. A.* **2005**, *102*, 11600.
(20) Bianco, A.; Prato, M. *Adv. Mater.* **2003**, *15*, 1765.
(21) Yang, W. R.; Thordarson, P.; Gooding, J. J.; Ringer, S. P.; Braet, F. *Nanotechnology* **2007**, *18*, 412001.
(22) Karajanagi, S. S.; Yang, H. C.; Asuri, P.; Sellitto, E.; Dordick, J. S.; Kane, R. S. *Langmuir* **2006**, *22*, 1392.
(23) Matsuura, K.; Saito, T.; Okazaki, T.; Ohshima, S.; Yumura, M.; Iijima, S. *Chem. Phys. Lett.* **2006**, *429*, 497.
(24) Lin, Y.; Allard, L. F.; Sun, Y. P. *J. Phys. Chem. B* **2004**, *108*, 3760.
(25) Kim, Y. S.; Cho, J. H.; Ansari, S. G.; Kim, H. I.; Dar, M. A.; Seo, H. K.; Kim, G. S.; Lee, D. S.; Khang, G.; Shin, H. S. *Synth. Met.* **2006**, *156*, 938.
(26) Gao, Y.; Kyratzis, I. *Bioconj. Chem.* **2008**, *19*, 1945.
(27) Wilchek, M.; Bayer, E. A. *Anal. Biochem.* **1988**, *171*, 1.
(28) Li, F. X.; Lu, Z. F.; Qian, H. T.; Rui, J. M.; Chen, S. N.; Jiang, P.; An, Y. L.; Mi, H. F. *Macromolecules* **2004**, *37*, 764.
(29) Li, F. X.; Liu, Z. F.; Liu, X. P.; Yang, X. Y.; Chen, S. N.; An, Y. L.; Zuo, J.; He, B. L. *Macromolecules* **2005**, *38*, 69.
(30) Cobbe, S.; Connolly, S.; Ryan, D.; Nagle, L.; Eritja, R.; Fitzmaurice, D. *J. Phys. Chem. B* **2003**, *107*, 470.
(31) Connolly, S.; Fitzmaurice, D. *Adv. Mater.* **1999**, *11*, 1202.
(32) Connolly, S.; Cobbe, S.; Fitzmaurice, D. *J. Phys. Chem. B* **2001**, *105*, 2222.
(33) Goux-Capes, L.; Filoramo, A.; Cote, D.; Bourgoin, J. P.; Patillon, J. N. *Phys. Status Solidi A* **2006**, *203*, 1132.
(34) Smorodin, T.; Beierlein, U.; Kotthaus, J. P. *Nanotechnology* **2005**, *16*, 1123.
(35) Chen, Z.; Tabakman, S. M.; Goodwin, A. P.; Kattah, M. G.; Daranciang, D.; Wang, X. R.; Zhang, G. Y.; Li, X. L.; Liu, Z.; Utz, P. J.; Jiang, K. L.; Fan, S. S.; Dai, H. J. *Nat. Biotechnol.* **2008**, *26*, 1285.
(36) Liu, Y.; Wang, Y. X.; Jin, J. Y.; Wang, H.; Yang, R. H.; Tan, W. H. *Chem. Commun.* **2009**, *6*, 665.
(37) Pantarotto, D.; Briand, J. P.; Prato, M.; Bianco, A. *Chem. Commun.* **2004**, *1*, 16.
(38) Hu, H.; Bhowmik, P.; Zhao, B.; Hamon, M. A.; Itkis, M. E.; Haddon, R. C. *Chem. Phys. Lett.* **2001**, *345*, 25.
(39) Wang, Z. W.; Shirley, M. D.; Meikle, S. T.; Whitby, R. L. D.; Mikhalovsky, S. V. *Carbon* **2009**, *47*, 73.
(40) Bradford, M. M. *Anal. Biochem.* **1976**, *72*, 248.
(41) Park, T. J.; Banerjee, S.; Hemraj-Benny, T.; Wong, S. S. *J. Mater. Chem.* **2006**, *16*, 141.
(42) Hu, H.; Yu, A. P.; Kim, E.; Zhao, B.; Itkis, M. E.; Bekyarova, E.; Haddon, R. C. *J. Phys. Chem. B* **2005**, *109*, 11520.
(43) Zhang, J.; Zou, H. L.; Qing, Q.; Yang, Y. L.; Li, Q. W.; Liu, Z. F.; Guo, X. Y.; Du, Z. L. *J. Phys. Chem. B* **2003**, *107*, 3712.
(44) Tchoul, M. N.; Ford, W. T.; Lolli, G.; Resasco, D. E.; Arepalli, S. *Chem. Mater.* **2007**, *19*, 5765.
(45) Balasubramanian, K.; Burghard, M. *Small* **2005**, *1*, 180.
(46) Ebner, A.; Wildling, L.; Zhu, R.; Rankl, C.; Haselgrubler, T.; Hinterdorfer, P.; Gruber, H. J. *STM and AFM Studies on (Bio)Molecular Systems: Unravelling the Nanoworld* **2008**, *285*, 29.
(47) Czajkowsky, D. M.; Shao, Z. *J Microsc.* **2003**, *211*, 1.
(48) Tomonari, Y.; Murakami, H.; Nakashima, N. *Chem.−Eur. J.* **2006**, *12*, 4027.
(49) Horcas, I.; Fernandez, R.; Gomez-Rodriguez, J. M.; Colchero, J.; Gomez-Herrero, J.; Baro, A. M. *Rev. Sci. Instrum.* **2007**, *78*, 13705.

JP911441D